García-Gutiérrez, A., Cubas, J., Chen, H., & Sanz-Andrés, Á. (2020).
Complex variable methods for linearized Euler rigid body rotation equations.
Acta Astronautica, 170, 454-465.

Complex Variable Methods for Linearized Euler Rigid Body Rotation Equations

Adrián García-Gutiérrez[a,*], Javier Cubas[b], Huan Chen[c], Ángel Sanz-Andrés[b]

[a] *Universidad de León, Aerospace Engineering Area, Campus de Vegazana S/n, León, 24071, Spain*
[b] *Instituto Universitario de Microgravedad 'Ignacio da Riva' (IDR/UPM), ETSIAE, Pza. del Cardenal Cisneros 3, Madrid, 28040, Spain.*
[c] *School of Astronautics, Beihang University, No.37, Xueyuan Road, Haidian District, Beijing, 100191, China*

Abstract

The determination of analytical solutions is a vital step in understanding the different physical systems and building confidence in the numerical methods that are required for more complex models. In the present work, analytical solutions are derived for axisymmetric and near-axisymmetric rigid body problems. The formulation proposed is based on a complex variable which characterizes all the different kinds of problems in similar terms. The described methodology is introduced for simple cases and, progressively, extended to other advanced problems such as random perturbations. As an application, this complex variable formulation can be used to characterize the asteroid' motions, showing a dependence between their inertia coefficients and their rotational velocities when the asteroid is perturbed from its relaxed state. A Montecarlo experiment is done in order to determine how well the inertia ratios of the asteroid can be estimated knowing only information about its angular velocities.

Contents

*Corresponding author
Email address: agarcg@unileon.es (Adrián García-Gutiérrez)

García-Gutiérrez, A., Cubas, J., Chen, H., & Sanz-Andrés, Á. (2020).
Complex variable methods for linearized Euler rigid body rotation equations.
Acta Astronautica, 170, 454-465.

Nomenclature

A, B, C	Principal moments of inertia
CDF	Cumulative Density Function

García-Gutiérrez, A., Cubas, J., Chen, H., & Sanz-Andrés, Á. (2020).
Complex variable methods for linearized Euler rigid body rotation equations.
Acta Astronautica, 170, 454-465.

DAMIT	Database of Asteroid Models from Inversion Techniques
FFT	Fast Fourier Transform
I	Parameter defined for a quasi-cylindrical inertia tensor as $I = \frac{A+B}{2}$
I_{13}	Inertia ratio $\frac{I_1}{I_3}$
I_{23}	Inertia ratio $\frac{I_2}{I_3}$
I_{13e}	Estimated inertia ratio $\frac{I_1}{I_3}$
I_{23e}	Estimated inertia ratio $\frac{I_2}{I_3}$
i	Imaginary unit
$\mathrm{Im}[x]$	Imaginary part of x
k	Parameter defined as $\omega_{30} t_c \frac{C-A}{A}$
k_0	Parameter defined as $\frac{C-A}{A}$
k_1	Parameter defined as $\omega_{30} t_c \frac{C-B}{A}$
k_2	Parameter defined as $\omega_{30} t_c \frac{C-A}{B}$
k_c	Parameter defined as $\sqrt{k_1 k_2}$
k_m	Parameter defined as $\sqrt{k_2/k_1}$
l_s, s_s	Major and minor semi-axes
m_1, m_2, m_3	Body-fixed Torques
M_{12}	Moment complex variable, $\frac{m_1+\mathrm{i}m_2}{A}$
$\mathrm{Re}[x]$	Real part of x
$S_{M_{12}}$	Spectral density of M_{12}
$S_{W_{12}}$	Spectral density of W_{12}
T	Dimensionless time, $T = \frac{t}{t_c}$
YORP effect	Yarkovsky-O'Keefe-Radzievskii-Paddack effect
W_{12}	Complex angular velocity, $\omega_1 + \mathrm{i}\omega_2$
α_1, α_2	Parameters use for the change of variable $\Omega_i = \alpha_i \overline{\Omega}_i$
$\delta\omega_i$	Small perturbation of ω_i
ϵ	Misalignment angle/perturbation parameter
θ, ϕ, ξ	Euler angles
θ_{12}	Complex variable defined as $\theta \mathrm{e}^{-\mathrm{i}\phi}$
ω	Angular velocity

García-Gutiérrez, A., Cubas, J., Chen, H., & Sanz-Andrés, Á. (2020).
Complex variable methods for linearized Euler rigid body rotation equations.
Acta Astronautica, 170, 454-465.

Ω	First order perturbed angular velocity
τ	Independent variable for spinning-up manoeuvres defined as $\frac{m_3}{C}t + \omega_{30}$
Subscripts	
1, 2, 3	Body-fixed coordinates using body frame
0	Initial condition
Superscripts	
i	Order of the perturbation problem
$\widehat{x}$	Complex amplitude of x
$\dot{x}$	Time derivative
x^*	Complex conjugate
$x^{'}$	Dimensionless time derivative $\frac{\partial x}{\partial T}$
$\overline{\Omega_i}$	Change of variable defined as $\Omega_i = \alpha_i \overline{\Omega}_i$

1. Introduction.

The lack of linearity presented in the real world phenomena is one of the major obstacles that engineers find when they are trying to model it. Although, in many cases, it is possible to know the equations which govern a particular problem, the complexity caused by this non-linearity prevents us from using an analytical approach to obtain the solutions. In these circumstances, the numerical methods can achieve a precise enough solution. However, this is done without gaining a valuable, significant knowledge about the physical driving process. It is for this reason that the analytical solution deserves the pertinent attention. Furthermore, analytical solutions are powerful tools for verifying and studying the errors originated by the numerical methods [1, 2].

The present work focus on the study of the rigid body rotation using the

García-Gutiérrez, A., Cubas, J., Chen, H., & Sanz-Andrés, Á. (2020).
Complex variable methods for linearized Euler rigid body rotation equations.
Acta Astronautica, 170, 454-465.

Euler's rotation equations [3]:

$$A\dot{\omega}_1 + \omega_2\omega_3(C - B) = m_1, \tag{1a}$$

$$B\dot{\omega}_2 + \omega_1\omega_3(A - C) = m_2, \tag{1b}$$

$$C\dot{\omega}_3 + \omega_1\omega_2(B - A) = m_3, \tag{1c}$$

where A, B and C are the principal moments of inertia about axes 1, 2 and 3 respectively. In these equations, the rotation of the body is studied using a rotating reference frame with its axes fixed to the body and parallel to the body's principal axes of inertia, see Figure 1. The angular velocities around the principal axes are ω_1, ω_2 and ω_3.

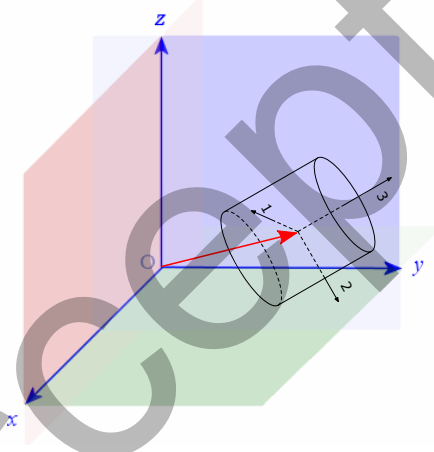

Figure 1: Instead of using an inertial reference frame xyz, the Euler equations are referred to body fixed principal axes of inertia 123.

Although these equations are well-known, the non linearity of the second term complicates the search for analytical solutions. Therefore, in many cases, the numerical solutions are the only viable method to solve the problem.

The general purpose of the present work is to simplify the analytic treatment of the rigid body dynamics and show the possibility of determining, in a simple and unified way, the rotational dynamics of bodies with an axisymmetric inertia tensor, which is useful from a view of both theoretical research and aerospace applications.

García-Gutiérrez, A., Cubas, J., Chen, H., & Sanz-Andrés, Á. (2020).
Complex variable methods for linearized Euler rigid body rotation equations.
Acta Astronautica, 170, 454-465.

Indeed, there are a set of problems in this field (torque free motion, stability of rotation, thrust misalignment, etc) whose analysis is generally presented in a case by case basis, which makes the whole presentation more complex and intricate. However, all these situations can be treated using the same basic tools, as will be shown in this paper.

The unified approach here proposed, reduces the work needed to explain the set of problems and the effort to understand the solutions, which, in this way, are naturally related to each other. This unified approach is based on the mathematical structure of the Euler equation when the inertia tensor is totally or nearly axisymmetric. In this case, the Euler equations become linear with regard to the transversal rotational speeds and the motion around the longitudinal axis is decoupled (if the external moments fulfill some conditions).

The structure of the paper is as follows. In Section 2, different axisymmetric problems that are common in aerospace engineering are described. These problems can be studied using complex variable as it is described in Section 3. In Section 4, the complex variable is applied to the different problems of Section 2. The methodology described is also extended to more general problems, including the non axisymmetric case, in Section 5, and it is applied to the movement of asteroids in Section 6. Finally, the conclusions are summarized in Section 7.

2. Common axisymmetric problems.

There are certain situations in aerospace engineering in which axisymmetric problems appear naturally. Some of them are described below.

2.1. Body with $A = B$ and zero external moment.

This is the simplest axisymmetric problem, where the rigid body is symmetric along axis 3 (without loss of generality) and there is no external torque.

García-Gutiérrez, A., Cubas, J., Chen, H., & Sanz-Andrés, Á. (2020).
Complex variable methods for linearized Euler rigid body rotation equations.
Acta Astronautica, 170, 454-465.

Then Eq. (1) can be simplified, with $A = B$ and $m_1 = m_2 = m_3 = 0$ as:

$$A\dot{\omega}_1 + \omega_2\omega_3(C - A) = 0, \tag{2a}$$

$$A\dot{\omega}_2 + \omega_1\omega_3(A - C) = 0, \tag{2b}$$

$$C\dot{\omega}_3 = 0. \tag{2c}$$

In this situation, the velocity around the axis of symmetry is decoupled from the other two. Typically, these equations can be used to model the movement of an axisymmetric spacecraft in the outer space. In that case, for a limited time interval, the external perturbations can be neglected. In general, these perturbations can be associated with inertial forces, tides, applied torques or the Yarkovsky-O'Keefe-Radzievskii-Paddack (YORP) effect [4], which is a change in the rotation rate caused by the asymmetric reflection and thermal re-radiation of sunlight from an irregularly shaped body [5].

2.2. Stability of rotation about principal axis.

It is known that permanent rotations are possible about each one of the principal axes [6]. To study the stability of rotation about the symmetry axis, axis 3, let us assume as initial condition $\omega_1 = \omega_2 = 0$, $\omega_3 = \omega_{30}$ and a perturbed condition so ω_1, $\omega_2 << \omega_{30}$ and $\omega_3 = \omega_{30} + \varepsilon$. Linearising equations (1) with $m_1 = m_2 = m_3 = 0$, the following equations are obtained:

$$A\dot{\omega}_1 + (C - A)\omega_2\omega_{30} = 0, \tag{3a}$$

$$B\dot{\omega}_2 + (A - C)\omega_1\omega_{30} = 0, \tag{3b}$$

$$C\dot{\omega}_3 = 0. \tag{3c}$$

2.3. Thrust misalignment.

This problem is another typical axisymmetric problem. As shown in [3], a spinning missile with a misalignment of the thrust line can be modeled in the following way: the missile is assumed axisymmetric so that the x, y, z axes coincide with the principal axes: 1, 2 and 3, with $I_1 = I_2 = A$, $I_3 = C$. Axis

García-Gutiérrez, A., Cubas, J., Chen, H., & Sanz-Andrés, Á. (2020).
Complex variable methods for linearized Euler rigid body rotation equations.
Acta Astronautica, 170, 454-465.

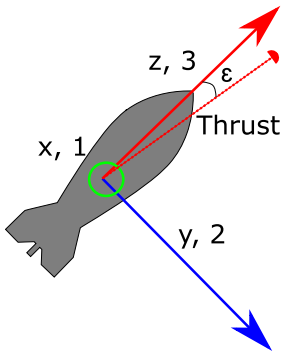

Figure 2: Reference system for the case of thrust misalignment. ϵ, misalignment angle.

1 is perpendicular to the thrust containing symmetry plane, and axis 3 is the revolution symmetry axis as shown in Figure 2.

The Euler's equations for the missile motion are:

$$A\dot{\omega}_1 + \omega_2\omega_3(C - A) = m_1, \tag{4a}$$

$$A\dot{\omega}_2 + \omega_1\omega_3(A - C) = 0, \tag{4b}$$

$$C\dot{\omega}_3 = 0, \tag{4c}$$

in which m_1 refers to the perturbation moment, independent of time and caused by the misalignment.

3. Use of the complex variable in axisymmetric problems.

In the case of an axisymmetric rigid solid, when axis 3 is the axis of symmetry, Eqs. (1) are simplified to:

$$A\dot{\omega}_1 + (C - A)\omega_2\omega_3 = m_1, \tag{5a}$$

$$A\dot{\omega}_2 + (A - C)\omega_1\omega_3 = m_2, \tag{5b}$$

$$C\dot{\omega}_3 = m_3. \tag{5c}$$

where $A = B$.

García-Gutiérrez, A., Cubas, J., Chen, H., & Sanz-Andrés, Á. (2020).
Complex variable methods for linearized Euler rigid body rotation equations.
Acta Astronautica, 170, 454-465.

It can be realized that when $A = B$ and m_3 fulfills some conditions (i.e, m_3 is independent of ω_1, ω_2) the dynamics of rotation around axis 3 is decoupled from rotations ω_1 and ω_2 [7]. Actually, from (1c), the velocity around the third axis can be calculated from:

$$\dot{\omega}_3 = \frac{m_3(t)}{C}. \tag{6}$$

If the solution of (6) can be obtained as $\omega_3(t)$, which means $m_3 = m_3(\omega_3, t)$, then Eqs. (5a) and (5b) can be solved by using the complex variable W_{12} defined in [6] as:

$$W_{12} = \omega_1 + \mathrm{i}\,\omega_2. \tag{7}$$

By adding Eqs. (5a) and (5b) in quadrature [6], the two equations are replaced by one in terms of the complex variable W_{12}:

$$\dot{W}_{12} - \mathrm{i}\,k\omega_3 W_{12} = M_{12}, \tag{8}$$

where the new variables k and M_{12} can be calculated from:

$$k = \frac{C - A}{A}, \tag{9a}$$

$$M_{12} = \frac{m_1 + \mathrm{i}\,m_2}{A}. \tag{9b}$$

The above method can be used not only in the situation of an axysimmetric body (which gives the exact solution for that case) but also when the product of ω_1 and ω_2 is very small [8]. The main advantage of equation (8) is its linearity. Its solutions can be easily obtained and, therefore, the problems presented in Section 2 and others of interest can be derived at once, as it is shown in what follows.

3.1. Rotations referred to inertial coordinates.

The determination of the motion using inertial coordinates are required in different kinds of situations like sun-tracking attitude motion [9]. Complex variable can also be useful in the case that the nutation angle θ is small enough.

García-Gutiérrez, A., Cubas, J., Chen, H., & Sanz-Andrés, Á. (2020).
Complex variable methods for linearized Euler rigid body rotation equations.
Acta Astronautica, 170, 454-465.

In that case, the classical solution for the rotation angles referred to inertial coordinates [3] are obtained from:

$$\omega_1 = \dot{\psi}\sin\theta\sin\varphi + \dot{\theta}\cos\varphi, \tag{10a}$$

$$\omega_2 = \dot{\psi}\sin\theta\cos\varphi - \dot{\theta}\sin\varphi, \tag{10b}$$

$$\omega_3 = \dot{\psi}\cos\theta + \dot{\varphi}, \tag{10c}$$

which relate rotation velocity components with Euler's angles θ, φ, ψ using a 3-1-3 sequence. A graphical representation of these angles can be seen in Figure 3.

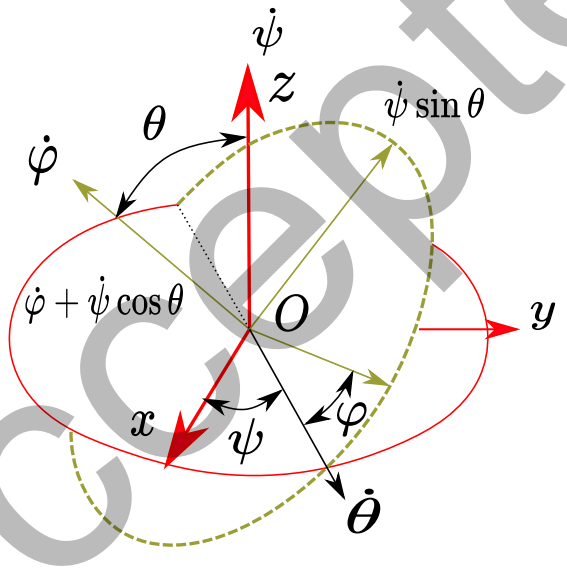

Figure 3: Angular rates of Euler angles.

By following the procedure explained in [3], the complex variable θ_{12} is defined as:

$$\theta_{12} = \theta\, \mathrm{e}^{-\mathrm{i}\,\varphi}\,. \tag{11}$$

When the new variable is used in Eq. (10), the coming expression is obtained:

$$\dot{\theta}_{12} + \mathrm{i}\,\omega_{30}\theta_{12} = W_{12}(t), \tag{12}$$

García-Gutiérrez, A., Cubas, J., Chen, H., & Sanz-Andrés, Á. (2020).
Complex variable methods for linearized Euler rigid body rotation equations.
Acta Astronautica, 170, 454-465.

where $\omega_{30} = \text{cte}$, considering the case $m_3 = 0$. In Eq. (12) W_{12} is known, as it is a solution of one of the above-mentioned problems. Eq. (12) is a linear ordinary differential equation with constant coefficients. This expression can be generalized for the cases referred to before, in which W_{12} is obtained as indicated and m_3 is not a constant but a function of time $m_3(t)$. In such a case, following the same procedure, a similar expression to (12) is obtained:

$$\dot{\theta}_{12} + \mathrm{i}\,\omega_3(t)\theta_{12} = W_{12}(t), \tag{13}$$

which is also a linear ordinary differential equation but with time-dependent coefficients. It should also be noted that while W_{12} is an exact solution, θ_{12} is only an approximation for small θ angles.

4. Solution of axisymmetric problems.

The problems presented in the previous section have analytical solutions when the variables meet certain conditions. Some of these solutions are well-known, as in the case of the thrust misalignment problem. In this section, a list of situations collected from the available literature is presented. The different problems, when they are written in terms of the complex variable, have analytical solutions. Without being totally exhaustive, this compilation can give the reader an idea of the kind of problems that can be addressed with this tool.

4.1. Body with zero external moment.

The zero external moment implies that $M_{12} = 0$ in (9b) and $\omega_3 = \omega_{30}$ in (6), where ω_{30} is the initial value of ω_3. Eq. (8) reduces to:

$$\dot{W}_{12} - \mathrm{i}\,k\omega_{30}W_{12} = 0, \tag{14}$$

whose solution is:

$$W_{12} = W_0\,\mathrm{e}^{\mathrm{i}\,k\omega_{30}t}, \tag{15}$$

where W_0 is a complex constant, $W_0 = \omega_1(0) + \mathrm{i}\omega_2(0)$, obtained from the initial conditions. Eq. (15) is the classical solution of the free body rotation.

García-Gutiérrez, A., Cubas, J., Chen, H., & Sanz-Andrés, Á. (2020).
Complex variable methods for linearized Euler rigid body rotation equations.
Acta Astronautica, 170, 454-465.

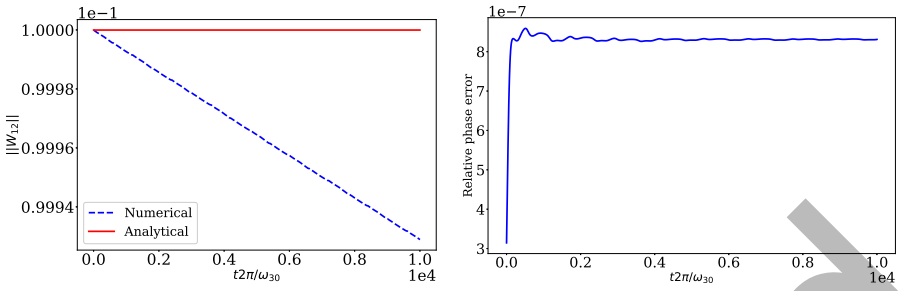

Figure 4: Comparison between numerical and analytical solutions for the case of a body with zero external moment. On the left, the absolute value of W_{12} is shown as a function of time. Although $|W_{12}| = W_0 = \text{cte}$, due to the errors in the numerical method, the absolute value decays. On the right, difference between the phase of W_{12} is shown as a function of time. Parameters: $A/C = B/C = 0.5$, $\omega_{10}/\omega_{30} = 0.1$, $\omega_{20}/\omega_{30} = 0$.

The difference between the numerical and analytical solutions is shown in Figure 4. The integration scheme is a Dormand & Price —member of the Runge–Kutta family— of order 8(5,3) —an 8th order scheme using a 5th order estimator with a 3th order correction.

As explained in a previous section, the complex variable also can be used for solving analytically the attitude of the body. Angle θ can be calculated using Eq. (13). An example of the solution using the analytical and numerical methods is shown in Figure 5. The difference between both methods is mostly due to linearization.

4.2. Constant transverse moments with zero axial moment.

In this case m_1 and m_2 are non-zero and $m_3 = 0$ (and, therefore, $\omega_3 = \omega_{30}$). An example of this case is the motion due to thrust misalignment. Eq. (8) can be written as:

$$\dot{W}_{12} - \mathrm{i}\, k\omega_{30} W_{12} = M_{12}. \tag{16}$$

Eq. (16) is a well known ordinary differential equation with constant coefficients, whose solution [10] is:

$$W_{12} = W_0\, \mathrm{e}^{\mathrm{i}\, k\omega_{30} t} + \frac{\mathrm{i}\, M_{12}}{k\omega_{30}} (1 - \mathrm{e}^{\mathrm{i}\, k\omega_{30} t}). \tag{17}$$

García-Gutiérrez, A., Cubas, J., Chen, H., & Sanz-Andrés, Á. (2020).
Complex variable methods for linearized Euler rigid body rotation equations.
Acta Astronautica, 170, 454-465.

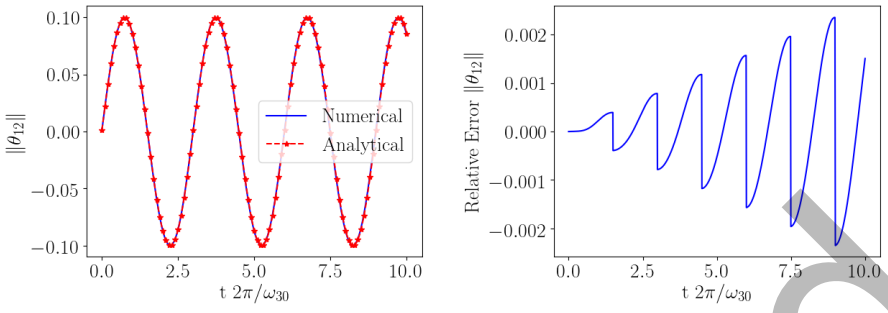

Figure 5: Comparison between numerical and analytical solutions in the case of rotations referred to inertial coordinates. On the left, absolute value of θ_{12} is shown as a function of time. On the right, error of θ_{12} as a function of time. Parameters: $A/C = B/C = 0.5$, $\omega_{10}/\omega_{30} = 0.1$, $\omega_{20}/\omega_{30} = 0$, $k_{12}/k_3 = 1$, $\theta_0 = 0.001$, $\varphi_0 = 0$, $\psi_0 = 0$ and zero external moments.

The physical meaning of the solution is that the attitude is determined by the combination of torque-free motion (15) and a driving term proportional to M_{12}.

4.3. Non-constant transversal moments with zero axial moment.

This case is a generalization of the previous one, where the complex moment M_{12} is a function of time, $M_{12}(t)$. Therefore Eq. (16) becomes

$$\dot{W}_{12} - \mathrm{i}\, k\omega_{30} W_{12} = M_{12}(t), \tag{18}$$

whose solution can be obtained by standard methods using the Laplace transformation:

$$W_{12} = W_0\, \mathrm{e}^{\mathrm{i}\, k\omega_{30} t} + \int_0^t M_{12}(\tau)\, \mathrm{e}^{\mathrm{i}\, k\omega_{30}(t-\tau)}\, \mathrm{d}\,\tau. \tag{19}$$

Similar to the previous case, solution (19) is a combination of the torque-free motion and the response to the driving torque $M_{12}(t)$ as it is shown in Figure 6.

García-Gutiérrez, A., Cubas, J., Chen, H., & Sanz-Andrés, Á. (2020).
Complex variable methods for linearized Euler rigid body rotation equations.
Acta Astronautica, 170, 454-465.

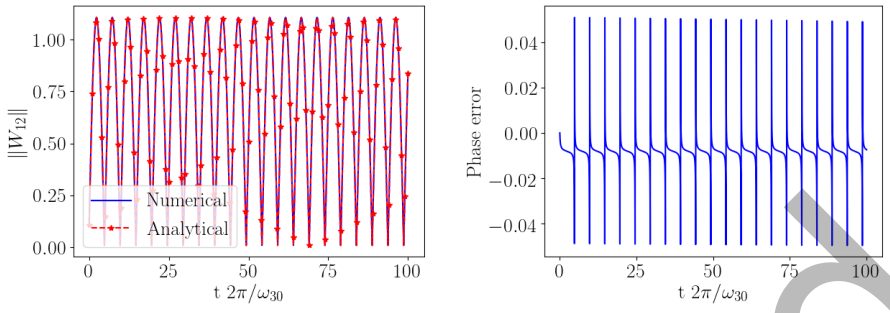

Figure 6: Comparison between numerical and analytical solution in the case of non-constant transversal moments with zero axial moment. On the left, the absolute value of W_{12} is shown as a function of time. 0n the right, the phase error of W_{12} is shown as a function of time. Parameters: $A/C = B/C = 0.5$, $\omega_{10}/\omega_{30} = 0.1$, $\omega_{20}/\omega_{30} = 0$, $M_{12}(t) = A\,\mathrm{e}^{\mathrm{i}\pi t/8}$.

4.4. Time-independent axial moment.

The spinning-up maneuvers can be treated as in [8] and [11], where ω_3 is approximated using its Taylor series expansion up to degree one:

$$\omega_3 = \frac{m_3}{C}t + \omega_{30}. \tag{20}$$

A new independent variable τ is defined as $\tau = \omega_3$. Once the variable change $\mathrm{d}t = C/m_3\ \mathrm{d}\tau$ is applied and after some substitutions, the following equation is obtained:

$$\dot{\Omega}_{12} - \mathrm{i}\,\tau\rho\Omega_{12} = M_{12}, \tag{21}$$

in which $\Omega_{12}{=}\omega_1\sqrt{B} + \mathrm{i}\,\omega_2\sqrt{A}$ and $\rho = \frac{C\sqrt{(C-A)(C-B)}}{m_3\sqrt{AB}}$. The solution of this equation is:

$$\Omega_{12} = \Omega_0\,\mathrm{e}^{\frac{1}{2}\mathrm{i}\,\rho\tau^2} + \int_0^\tau M_{12}(\xi)\,\mathrm{e}^{\frac{1}{2}\mathrm{i}\,\rho(\tau^2-\xi^2)}\,\mathrm{d}\,\xi. \tag{22}$$

García-Gutiérrez, A., Cubas, J., Chen, H., & Sanz-Andrés, Á. (2020).
Complex variable methods for linearized Euler rigid body rotation equations.
Acta Astronautica, 170, 454-465.

4.5. Moments with linear dependence on the rotation speed components.

Consider the case where m_1 and m_2 are linear functions of ω_1, ω_2, and ω_3 and m_3 is only a function of ω_3:

$$m_1 = m_1(\omega_1, \omega_2, \omega_3), \tag{23a}$$

$$m_2 = m_2(\omega_1, \omega_2, \omega_3), \tag{23b}$$

$$m_3 = m_3(\omega_3). \tag{23c}$$

From Eq. (6) one can obtain $\omega_3 = \omega_3(t)$ and by substituting it into (8):

$$\dot{W}_{12} - \mathrm{i}\, k\omega_3(t) W_{12} = M_{12}(W_{12}, W_{12}^*, \omega_3), \tag{24}$$

where W_{12}^* is the complex conjugate of W_{12}.

The analytical integration of (24) can be performed in some cases [12]. As an example, let us consider the case where the external torque is a linear damping, which can be modeled as follows:

$$m_1 = -k_1 \omega_1 A, \tag{25a}$$

$$m_2 = -k_2 \omega_2 A, \tag{25b}$$

$$m_3 = -k_3 \omega_3 C. \tag{25c}$$

If $k_1 = k_2 = k_{12}$, from (9b) and (24), we can obtain:

$$M_{12} = -k_{12} W_{12}, \tag{26a}$$

$$\dot{W}_{12} - \mathrm{i}\, k\omega_3(t) W_{12} = -k_{12} W_{12}. \tag{26b}$$

The solution of (6) using (25c) is:

$$\omega_3(t) = \omega_{30}\, \mathrm{e}^{-k_3 t} = \omega_{30}\, \mathrm{e}^{-t/t_{c3}}, \tag{27}$$

which represents an exponential decay with characteristic time $t_{c3} = \frac{1}{k_3}$, during which the value of ω_3 has been reduced approximately a 63%.

Eq. (26b) together with Eq. (27) becomes:

$$\dot{W}_{12} - [k_{12} - \mathrm{i}\, k_{12}\omega_{30}\, \mathrm{e}^{-t/t_{c3}}] W_{12} = 0, \tag{28}$$

García-Gutiérrez, A., Cubas, J., Chen, H., & Sanz-Andrés, Á. (2020).
Complex variable methods for linearized Euler rigid body rotation equations.
Acta Astronautica, 170, 454-465.

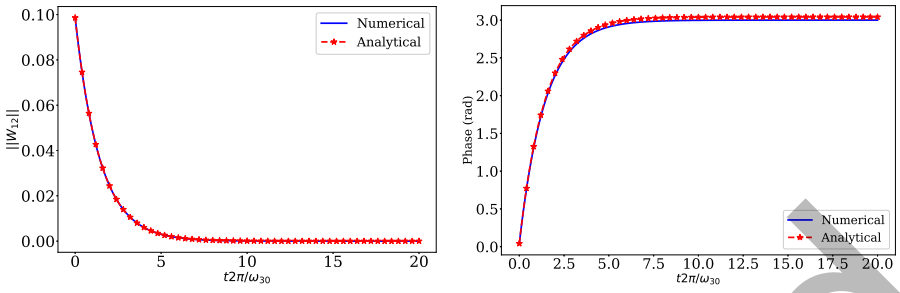

Figure 7: Comparison between numerical and analytical solution in the case of moments with linear dependence on the rotation speed components. On the left, the absolute value of W_{12} is shown as a function of time. The exponential decay of the absolute value is clear, which causes that both solutions reach the same final value. On the right, the phase of W_{12} as a function of time. Parameters: $A/C = B/C = 0.5$, $\omega_{10}/\omega_{30} = 0.1$, $\omega_{20}/\omega_{30} = 0$, $k_{12}/k_3 = 1$.

whose solution is given by

$$W_{12}(t) = W_0 e^{-k_{12}t}\, \mathrm{e}^{\mathrm{i}\, g(t)}, \tag{29}$$

where:

$$g(t) = k \int \omega_3(t)\, \mathrm{dt} = k\omega_{30} t_{c3}(1 - \mathrm{e}^{-t/t_{c3}}), \tag{30}$$

and $t_{c3} = 1/k_3$. The constant in (30) has been arbitrarily selected to fulfill the condition $g(0) = 0$ —i.e., $\omega_2(0) = 0$— without lose of generality.

The solution W_{12} (see Figure 7) is composed of two factors. The first one $\mathrm{e}^{-k_{12}t}$ represents the decay of the transverse rotation speed components amplitude with a time scale $1/k_{12}$. The second factor is a unitary vector which represents the two harmonic components of a rotating vector whose angular speed is:

$$\Omega(t) = \frac{k\omega_{30} t_{c3}(1 - \mathrm{e}^{-t/t_{c3}})}{t} = \frac{g(t)}{t}, \tag{31}$$

and therefore changes with time. The rate of change is determined by the characteristic time t_{c3}. As an example, for times $t << t_{c3}$ the angular speed can be approximated, by neglecting larger order terms, as:

$$\Omega(t) \approx k\omega_{30}\left[1 - \frac{t}{2t_{c3}}\right], \tag{32}$$

García-Gutiérrez, A., Cubas, J., Chen, H., & Sanz-Andrés, Á. (2020).
Complex variable methods for linearized Euler rigid body rotation equations.
Acta Astronautica, 170, 454-465.

which shows that the initial value of the angular speed of vector W_{12} is $k\omega_{30}$ and this speed decreases with characteristic time t_{c3}.

The angle, θ, between the angular velocity vector and the symmetry axis (axis 3) can be obtained with equations (27) and (29) and is given by:

$$\tan\theta = \frac{|W_0|}{\omega_{30}}\frac{A}{C}\,\mathrm{e}^{(-k_{12}+k_3)t}\,. \tag{33}$$

It is shown that the angular velocity vector changes its position with regard to axis 3 due to the change in angular momentum caused by the external torque (m_1, m_2, m_3). The rate of change is determined by the characteristic time $\frac{1}{|k_{12}-k_3|}$ and the change of direction (increase or decrease) is determined by the sign of the difference $k_{12} - k_3$.

5. Generalized problem.

Although the above examples may seem very specific, the complex variable has shown utility and can be applied to more general cases. In this section the authors present methods for applying this tool to quasi-axilsymmetric bodies and more general disturbances.

5.1. Time-dependent moments.

This case is more general than the previous ones. ω_3 can be calculated integrating the equation (6)[13], with initial condition ω_{30}, that is:

$$\omega_3 = \omega_{30} + \frac{1}{C}\int_0^t m_3(t), \tag{34}$$

which introduced into (8) gives:

$$\dot{W}_{12} - \mathrm{i}\,k\omega_3(t)W_{12} = M_{12}(t). \tag{35}$$

Eq. (35) is a linear differential equation with time-dependent coefficients whose solution can be obtained by standard methods [14].

García-Gutiérrez, A., Cubas, J., Chen, H., & Sanz-Andrés, Á. (2020).
Complex variable methods for linearized Euler rigid body rotation equations.
Acta Astronautica, 170, 454-465.

5.2. Response to harmonic or random inputs.

There are situations in which the inputs are known to be periodic and can be decomposed into harmonics. This is the case, for example, when studying a sun-synchronous frozen orbit [9]. In this case, the solutions of Eqs. (6) and (8) are found when $m_1(t), m_2(t), m_3(t)$ are harmonic or random functions of time.

Let us consider the definition of variables ω_3, m_3, W_{12} and M_{12}:

$$\omega_3 = \widehat{\omega}_3(\omega)\, \mathrm{e}^{\mathrm{i}\,\omega t} + \omega_{30}, \tag{36a}$$

$$m_3 = \widehat{m}_3(\omega)\, \mathrm{e}^{\mathrm{i}\,\omega t}, \tag{36b}$$

$$W_{12} = \widehat{W}_{12}(\omega)\, \mathrm{e}^{\mathrm{i}\,\omega t}, \tag{36c}$$

$$M_{12} = \widehat{M}_{12}\, \mathrm{e}^{\mathrm{i}\,\omega t}, \tag{36d}$$

where $\widehat{\omega}_3, \widehat{m}_3, \widehat{W}_{12}, \widehat{M}_{12}$ are the complex amplitudes, function of the angular frequency, ω, and ω_{30} is a constant.

Solution of (6) gives the following relationship between $\widehat{\omega}_3$ and $\widehat{\omega}_{30}$:

$$\widehat{\omega}_3(\omega) = \frac{\widehat{m}_3(\omega)}{\mathrm{i}\,\omega C}, \tag{37}$$

when introduced in (8) leads to:

$$\widehat{W}_{12}(\omega) = \frac{\widehat{M}_{12}(\omega)}{\mathrm{i}\,\omega - \mathrm{i}\,k\left[\omega_{30} + \frac{\widehat{m}_3(\omega)}{\mathrm{i}\,\omega C}\,\mathrm{e}^{\mathrm{i}\,\omega t}\right]}. \tag{38}$$

In order for the solution (38) to be a harmonic one, the condition $\widehat{m}_3(\omega) = 0$ should be fulfilled, and therefore Eq. (38) reduces to:

$$\widehat{W}_{12}(\omega) = \frac{\mathrm{i}}{k\omega_{30} - \omega}\widehat{M}_{12}(\omega), \tag{39}$$

which shows the possibility of a resonant response when the angular frequency ω fulfills the condition $\omega = \omega_{30}$. The factor i denotes the quadrature between the torque and the rotation speed.

In the case of a random input, Eq. (39) can be used to define the relationship between the spectral density of the input —the torque $\widehat{M}_{12}(\omega)$— and of the output —the transverse rotation speed $\widehat{W}_{12}(\omega)$:

$$S_{W_{12}}(\omega) = \frac{S_{M12}(\omega)}{(k\omega_{30} - \omega)^2}, \tag{40}$$

García-Gutiérrez, A., Cubas, J., Chen, H., & Sanz-Andrés, Á. (2020).
Complex variable methods for linearized Euler rigid body rotation equations.
Acta Astronautica, 170, 454-465.

where $S_{W_{12}}$and $S_{M_{12}}$ are the spectral densities of the transverse rotation speed and of the external transverse torque, respectively. Eq. (39) allows us to determine the variance of the transverse rotation speed modulus from the spectral density of the transverse torque. In order to do so, some damping should be introduced into Eq. (38) to manage the response in the resonant range.

5.3. Quasi-cylindrical inertia tensor.

It is also possible to relax the axilsymmetry requirement for the rigid solid. Let us consider the case where the inertia tensor is quasi-cylindrical, $|A-B| << A$. Therefore, the magnitudes of the problem can be expressed in the following way:

$$A = I(1-\epsilon), \tag{41a}$$

$$B = I(1+\epsilon), \tag{41b}$$

$$k_0 = \frac{C-I}{I}, \tag{41c}$$

$$I = \frac{A+B}{2}, \tag{41d}$$

$$\epsilon = \frac{B-A}{B+A}, \tag{41e}$$

$$\omega_i = \omega_i^0 + \epsilon\omega_i^1, \tag{41f}$$

with $\epsilon \ll 1$.

By introducing (41) into (1c), one obtains the following equation:

$$\dot{\omega}_3^0 + \epsilon\dot{\omega}_3^1 + 2\epsilon\frac{I}{C}(\omega_1^0 + \epsilon\omega_1)(\omega_2^0 + \epsilon\omega_2) = \frac{m_3}{C}, \tag{42}$$

which leads to the following equations for ω_3^0:

$$\dot{\omega}_3^0 = \frac{m_3}{C}, \tag{43}$$

and ω_3^1:

$$\dot{\omega}_3^1 = -2\frac{I}{C}\omega_1^0\omega_2^0. \tag{44}$$

By introducing (41) into Eqs.(1a) and (1b), the Taylor expansion can be

García-Gutiérrez, A., Cubas, J., Chen, H., & Sanz-Andrés, Á. (2020).
Complex variable methods for linearized Euler rigid body rotation equations.
Acta Astronautica, 170, 454-465.

applied obtaining:

$$\dot{\omega}_1 + k_0\omega_2\omega_3 - \epsilon(1-k_0)\omega_2\omega_3 = \frac{m_1}{I}(1+\epsilon), \tag{45a}$$

$$\dot{\omega}_2 - k_0\omega_1\omega_3 - \epsilon(1-k_0)\omega_1\omega_3 = \frac{m_2}{I}(1-\epsilon). \tag{45b}$$

Adding (45a) and (45b) in quadrature leads to:

$$\dot{\omega}_1 + \mathrm{i}\,\dot{\omega}_2 + k_0\omega_3(\omega_2 - \mathrm{i}\,\omega_1) - \epsilon(1-k_0)\omega_3(\omega_2 + \mathrm{i}\,\omega_1) = \frac{m_1 + \mathrm{i}\,m_2 + \epsilon(m_1 - \mathrm{i}\,m_2)}{I}, \tag{46}$$

or:

$$\dot{W}_{12} - \mathrm{i}\,k_0\omega_3 W_{12} - \mathrm{i}\,\epsilon(1-k_0)\omega_3 W_{12}^* = \frac{M_{12} + \epsilon M_{12}^*}{I}. \tag{47}$$

To solve Eq. (47), let us consider the expansion:

$$W_{12} = W_{12}^0 + \epsilon W_{12}^1, \tag{48}$$

introducing it into (47) together with (41f) gives two expressions for the zero and first order problems as:

$$\dot{W}_{12}^0 - \mathrm{i}\,k_0\omega_3^0 W_{12}^0 = \frac{M_{12}}{I}, \tag{49a}$$

$$\dot{W}_{12}^1 - \mathrm{i}\,k_0\omega_3^0 W_{12}^1 = \frac{M_{12}^*}{I} + \mathrm{i}\,k_0\omega_3^1 W_{12}^0 + \mathrm{i}(1-k_0)\omega_3^0 W_{12}^{0*}, \tag{49b}$$

where:

$$W_{12}^i = \omega_1^i + \mathrm{i}\,\omega_2^i, \tag{50}$$

in which the superscript indicates the order of the problem.

The zero order problem (49a) is identical to the non-perturbed problem, $\varepsilon = 0$, that is, the forced motion of a body with axisymmetric inertia tensor. Although the first order problem (49b) has the same structure as the zero order problem, it changes the form of the right-hand side terms. As a consequence, the solution depends on the initial conditions and on the external torques grouped in the symbols m_3 and M_{12}.

5.4. Quasi-cylindrical inertia tensor and torque-free motion.

One case of basic interest is the torque-free motion ($m_1 = m_2 = m_3 = 0$) where the zero-order problem (34) and (49a) leads to $\omega_3^0 = \omega_{30}^0$, being $\omega_3^0 =$

García-Gutiérrez, A., Cubas, J., Chen, H., & Sanz-Andrés, Á. (2020).
Complex variable methods for linearized Euler rigid body rotation equations.
Acta Astronautica, 170, 454-465.

$\omega_{30}^0(0)$ a constant, and:

$$\dot{W}_{12}^0 - \mathrm{i}\, k_0 \omega_{30}^0 W_{12}^0 = 0. \tag{51}$$

The solution of (51) is:

$$W_{12}^0 = W_{120}^0\, \mathrm{e}^{\mathrm{i}\, k_0 \omega_{30}^0 t}, \tag{52}$$

where $W_{120}^0 = W_{12}^0(0)$ is the initial value of W_{12}^0. Under suitable conditions $W_{12}(0) = \omega_{120}^0$, and from (52) it is deduced:

$$\omega_1^0 = \mathrm{Re}\left[W^0\right] = \omega_{120}^0 \cos(k_0 \omega_{30}^0 t), \tag{53a}$$

$$\omega_2^0 = \mathrm{Im}\left[W^0\right] = \omega_{120}^0 \sin(k_0 \omega_{30}^0 t). \tag{53b}$$

The solution of the zero-order problem $(\omega_1^0, \omega_2^0, \omega_3^0)$ is the classical solution of the torque-free motion of a body with axisymmetric inertia tensor. In order to determine the first order correction, introduce (53) into (44) to obtain:

$$\dot{\omega}_3^1 = -2\frac{I}{C}(\omega_{120}^0)^2 \cos(k_0 \omega_{30}^0 t) \sin(k_0 \omega_{30}^0 t) = -\frac{I}{C}(\omega_{120}^0)^2 \sin(2k_0 \omega_{30}^0 t). \tag{54}$$

whose solution is:

$$\omega_3^1 = \frac{I}{C}\frac{(\omega_{120}^0)^2}{2k_0 \omega_{30}^0} \cos(2k_0 \omega_{30}^0 t), \tag{55}$$

which shows that the rotation around axis 3 is not performed at a constant rate. It is the result of the superposition of the zero order constant rotation ω_{30}^0 with ω_3^1 which has an amplitude of $\frac{I}{C}\frac{(\omega_{120}^0)^2}{2k_0\omega_{30}^0}$ and angular frequency of $2k_0\omega_{30}^0$. That frequency is the double of the angular frequency of W_{12}^0.

The first order term will introduce an angular acceleration which will produce a vibration of the body structure elements.

The transverse rotation speed correction W_{12}^1 is obtained from (49b), which reduces to:

$$\dot{W}_{12}^1 - \mathrm{i}\, k_0 \omega_3^0 W_{12}^1 = \mathrm{i}\, k_0 \omega_3^1 W_{12}^0 + \mathrm{i}(1-k_0)\omega_3^0 W_{12}^{0*}, \tag{56}$$

García-Gutiérrez, A., Cubas, J., Chen, H., & Sanz-Andrés, Á. (2020).
Complex variable methods for linearized Euler rigid body rotation equations.
Acta Astronautica, 170, 454-465.

together with (52) and (55), leading to the following expression:

$$\dot{W}_{12}^1 - \mathrm{i}\, k_0 \omega_{30}^0 W_{12}^1 = \mathrm{i}\, \frac{I}{C} \frac{(\omega_{120}^0)^3}{2\omega_{30}^0} \cos(2k_0\omega_{30}^0 t)\, \mathrm{e}^{\mathrm{i}k_0\omega_{30}^0 \mathrm{t}} + \mathrm{i}(1-k_0)\omega_{30}^0\omega_{120}^0\, \mathrm{e}^{-\,\mathrm{i}\,k_0\omega_{30}^0 t} =$$

$$= \mathrm{i}\, \frac{\omega_{120}^0}{\omega_{30}^0} \left[\frac{I}{2C} (\omega_{120}^0)^2 \cos(2k_0\omega_{30}^0 t)\, \mathrm{e}^{\mathrm{i}k_0\omega_{30}^0 \mathrm{t}} + (1-k_0)(\omega_{30}^0)^2\, \mathrm{e}^{-\,\mathrm{i}\,k_0\omega_{30}^0 t} \right]. \quad (57)$$

The solution of (57) with initial condition $W_{12}^1(0) = W_{120}^0$ is:

$$W_{12}^1(t) = W_{120}^1\, \mathrm{e}^{i\alpha t} + \frac{B}{\alpha} \sin(\alpha t) + \frac{A}{2\alpha} \sin(2\alpha t)\, \mathrm{e}^{\mathrm{i}\,\alpha t}, \quad (58)$$

where:

$$\alpha = k_0\omega_{30}^0, \quad (59a)$$

$$A = \mathrm{i}\, \frac{I}{C} \frac{(\omega_{120}^0)^3}{2\omega_{30}^0}, \quad (59b)$$

$$B = \mathrm{i}(1-k_0)\omega_{30}^0\omega_{120}^0. \quad (59c)$$

Therefore, the correction $W_{12}^0(t)$ for the transverse rotational speed is composed of harmonic terms with angular frequencies $k_0\omega_{30}^0$ and $2k_0\omega_{30}^0$ —coming from the term $\sin(2\alpha t)\mathrm{e}^{\mathrm{i}\,\alpha t}$.

5.5. Rotating non-cylindrical inertia tensor with small perturbation torques.

Finally, an example is presented where axilsymmetry is not needed, the case of small perturbations acting on a relaxed body rotating around the principal axis of inertia. The description of its motion using the Euler equations and integrating the inertia tensor for different cases could be complex. However, there is a simple case in which the inertia tensor is cylindrical [3] and the problem can be resolved using a change of variable to the complex domain. This method, for a cylindrical inertia tensor, can be generalized to non-cylindrical in the case of small perturbations. This is done with a change in the angular velocities scale.

The stable solution when $m_1 = m_2 = m_3 = 0$ is given by $\omega_3 = \omega_{30}$, $\omega_1 = \omega_2 = 0$. If the equilibrium state is perturbed with a small perturbation, the new

García-Gutiérrez, A., Cubas, J., Chen, H., & Sanz-Andrés, Á. (2020).
Complex variable methods for linearized Euler rigid body rotation equations.
Acta Astronautica, 170, 454-465.

solution is given by

$$\omega_3 = \omega_{30}(1 + \epsilon\Omega_3), \tag{60a}$$

$$\omega_2 = \epsilon\omega_{30}\Omega_2, \tag{60b}$$

$$\omega_1 = \epsilon\omega_{30}\Omega_1. \tag{60c}$$

Substituting Eqs. (60) into Eqs. (3), the new approximated equations are:

$$\dot{\Omega}_1 + \frac{C-B}{A}\Omega_2\omega_{30} = \frac{1}{\epsilon}\frac{m_1}{\omega_{30}A}, \tag{61a}$$

$$\dot{\Omega}_2 + \frac{A-C}{B}\Omega_1\omega_{30} = \frac{1}{\epsilon}\frac{m_2}{\omega_{30}B}, \tag{61b}$$

$$\dot{\Omega}_3 + \frac{B-A}{C}\Omega_1\Omega_2\omega_{30}\epsilon = \frac{1}{\epsilon}\frac{m_3}{\omega_{30}C}. \tag{61c}$$

The perturbations moments must be small enough in order to fulfill the condition that the right-hand side of the equations are first order perturbations. With all this, the equations (61a), (61b) are decoupled from (61c) and are linear. A dimensionless time T with $t = t_c T$ will be used where t_c is a characteristic time to be defined. Using $X' = \frac{\partial X}{\partial T}$, the dimensionless equations are:

$$\Omega_1' + \frac{C-B}{A}\Omega_2\omega_{30}t_c = \frac{1}{\epsilon}\frac{t_c}{\omega_{30}}\frac{m_1}{A}, \tag{62a}$$

$$\Omega_2' + \frac{A-C}{B}\Omega_1\omega_{30}t_c = \frac{1}{\epsilon}\frac{t_c}{\omega_{30}}\frac{m_2}{B}, \tag{62b}$$

$$\Omega_3' + \frac{B-A}{B}\Omega_1\Omega_2\omega_{30}t_c\epsilon = \frac{1}{\epsilon}\frac{t_c}{\omega_{30}}\frac{m_3}{C}. \tag{62c}$$

In the case of a symmetrical tensor, the problem is greatly simplified. With $k = \omega_{30}t_c\frac{C-A}{A} > 0$ and considering the homogeneous problem, one obtains:

$$\Omega_1' + k\Omega_2 = 0, \tag{63a}$$

$$\Omega_2' - k\Omega_1 = 0. \tag{63b}$$

Next, define a new complex variable W as:

$$W = \Omega_1 + \mathrm{i}\,\Omega_2, \tag{64}$$

García-Gutiérrez, A., Cubas, J., Chen, H., & Sanz-Andrés, Á. (2020).
Complex variable methods for linearized Euler rigid body rotation equations.
Acta Astronautica, 170, 454-465.

in a similar way as it had been done in [6].

Adding the equation (63a) to the equation (63b) in quadrature results in:

$$\Omega_1^{'} + \mathrm{i}\,\Omega_2^{'} + k(\Omega_2 - \mathrm{i}\,\Omega_1) = 0 \Rightarrow W^{'} - \mathrm{i}\,kW = 0. \tag{65}$$

Therefore, the solution to the problem is a spin of constant velocity k of the vector $W_0 = \Omega_{10} + \mathrm{i}\,\Omega_{20}$, as:

$$W = W_0\,\mathrm{e}^{\mathrm{i}\,kT}\,. \tag{66}$$

When there is no symmetry around the principal inertial axis, the case is more interesting. The method requires a transformation with $\Omega_i = \alpha_i \overline{\Omega}_i$ defining $k_1 = \omega_{30} t_c \frac{C-B}{A} > 0$ and $k_2 = \omega_{30} t_c \frac{C-A}{B} > 0$. The new equations are:

$$\overline{\Omega}_1^{'} + k_1 \frac{\alpha_2}{\alpha_1} \overline{\Omega}_2 = 0, \tag{67a}$$

$$\overline{\Omega}_2^{'} - k_2 \frac{\alpha_1}{\alpha_2} \overline{\Omega}_1 = 0. \tag{67b}$$

These equations can be transformed into (63a) and (63b) by choosing the values of α_1 and α_2 as:

$$k_1 \frac{\alpha_2}{\alpha_1} = k_2 \frac{\alpha_1}{\alpha_2} \implies \left(\frac{\alpha_2}{\alpha_1}\right)^2 = \frac{k_2}{k_1} = k_c^2, \tag{68a}$$

$$\alpha_1 = 1 \implies \alpha_2 = \sqrt{k_2/k_1} = k_c, \tag{68b}$$

$$k_1 k_c = \sqrt{k_1 k_2} = k_m. \tag{68c}$$

Values of α_1 and α_2 are arbitrary as long as Eq. (68a) is fulfilled. With these values, the following equations are obtained:

$$\overline{\Omega}_1^{'} + k_m \overline{\Omega}_2 = 0, \tag{69a}$$

$$\overline{\Omega}_2^{'} - k_m \overline{\Omega}_1 = 0. \tag{69b}$$

Therefore, changing the scale of amplitude of the traditional variables, the non-cylindrical problem is converted to a cylindrical one with a straightforward solution as:

$$\overline{W} = \overline{\Omega}_1 + \mathrm{i}\,\overline{\Omega}_2 = \Omega_1 + \frac{\mathrm{i}}{k_c}\Omega_2 \quad ; \quad \overline{W} = \overline{W}_0\,\mathrm{e}^{\mathrm{i}\,k_m T} \quad ; \quad \overline{W}_0 = \overline{\Omega}_{10} + \mathrm{i}\,\overline{\Omega}_{20} \tag{70}$$

García-Gutiérrez, A., Cubas, J., Chen, H., & Sanz-Andrés, Á. (2020).
Complex variable methods for linearized Euler rigid body rotation equations.
Acta Astronautica, 170, 454-465.

6. Study case: asteroids.

In this section an application of one of the previously proposed methods to a real problem is presented. As explained above, the axilsimmetry requirement is not essential for the application of the complex variable method. To illustrate this fact, a problem in which the body does not necessarily have axial symmetry has been chosen: the motion described by asteroids.

For the analysis, the low-amplitude rotations of asteroids are considered. They will be modeled as small perturbations around the principal axis of inertia [15]. The reason for this choice is the fact that observable asteroids are in a relaxed rotation state and low speed, because of the nutation relaxation [16], and the fact that large speed reduces their life. This dynamic is an example of the motion analyzed in Subsection 5.5.

The solution of this motion, equation (70), indicates that the vector $\overline{W}_0$ spins at a constant rate k_m —dimensionless— and the vector W moves following an ellipse with semiaxis $|\overline{W}_0|$ and $|\frac{\overline{W}_0}{k_c}|$, where $|\overline{W}_0|$ is the circumference radius that encloses the ellipse:

$$\Omega_1 \equiv \mathrm{Re}\left[W\right] = \overline{\Omega}_1 = \mathrm{Re}\left[\overline{W}_0\, \mathrm{e}^{\mathrm{i}\, k_m T}\right], \tag{71}$$

$$\Omega_2 \equiv \mathrm{Im}\left[W\right] = \frac{\overline{\Omega}_2}{k_c} = \frac{1}{k_c}\,\mathrm{Im}\left[\overline{W}_0\, \mathrm{e}^{\mathrm{i}\, k_m T}\right]. \tag{72}$$

Figure 8 shows the graphical interpretation of these results. The constants k_m and k_c can be computed from the observation of the asteroid movement.

On the other hand, both k_m and k_c can also be computed from the asteroid inertial matrix. From the relation of the ellipse semi-axis, k_c can be obtained as:

$$k_c = \sqrt{\frac{k_2}{k_1}} = \sqrt{\frac{C-A}{C-B}\frac{A}{B}} = \sqrt{\frac{1-I_{13}}{1-I_{23}}\frac{I_{13}}{I_{23}}} = \sqrt{a}, \tag{73}$$

where $I_{13} = A/C$ and $I_{23} = B/C$. A relationship between the spin velocity of the vector $\overline{W}$ with these ratios is given by:

García-Gutiérrez, A., Cubas, J., Chen, H., & Sanz-Andrés, Á. (2020).
Complex variable methods for linearized Euler rigid body rotation equations.
Acta Astronautica, 170, 454-465.

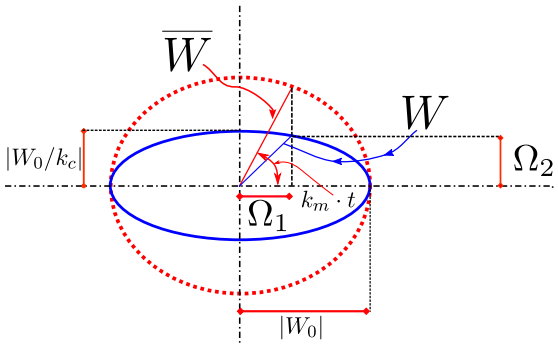

Figure 8: Trajectory of the complex rotation speed W and the stretched one $\overline{W}$.

$$\frac{k_m}{t_c} = \sqrt{\frac{k_1 k_2}{t_c^2}} = \sqrt{\frac{(C-B)(C-A)}{t_c^2}\frac{\omega_{30}^2 t_c^2}{AB}}$$
$$= \omega_{30}\sqrt{\frac{C-B}{A}\frac{C-A}{B}} = \omega_{30}\sqrt{\frac{1-I_{23}}{I_{13}}\frac{1-I_{13}}{I_{23}}} = \sqrt{b}\omega_{30}. \quad (74)$$

Rearranging equations (73) and (74) we can obtain:

$$a = \frac{(I_{13}-1)I_{13}}{(I_{23}-1)I_{23}}, \quad (75)$$

$$b = \frac{1-I_{23}}{I_{13}}\frac{1-I_{13}}{I_{23}}. \quad (76)$$

that can be used to calculate the possible values of I_{13} and I_{23} as:

$$I_{13} = \frac{-1 \pm \sqrt{ab}}{b-1}, \quad (77a)$$

$$I_{23} = \frac{-a \pm \sqrt{ab}}{a(b-1)}. \quad (77b)$$

The Eqs. (77a) and (77b) give two possible values for I_{13} and I_{23}, however, there are additional requirements that can be used to find the true solution. First, the inertia ratios must be a positive quantity. Second, the considered rotation movements are around the main inertial axis so, by definition, $I_3 > I_2 > I_1 > 0$. Both conditions imply that $0 < I_{13} < I_{23} < 1$. Figures 9 and 10 show the two possible values of I_{13} and I_{23} from Eqs. (77a) and (77b). However,

García-Gutiérrez, A., Cubas, J., Chen, H., & Sanz-Andrés, Á. (2020).
Complex variable methods for linearized Euler rigid body rotation equations.
Acta Astronautica, 170, 454-465.

if the condition $0 < I_{13} < I_{23} < 1$ is now applied, a unique solution is obtained: the one which has the positive sign before the root square.

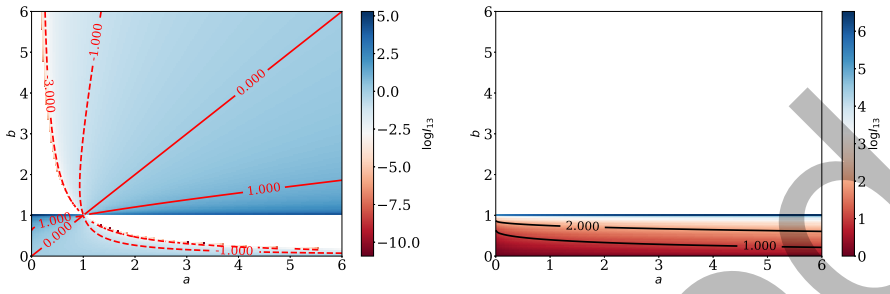

Figure 9: Logarithm of I_{13} for different a and b using the solution of sign "+" (left) and(right).

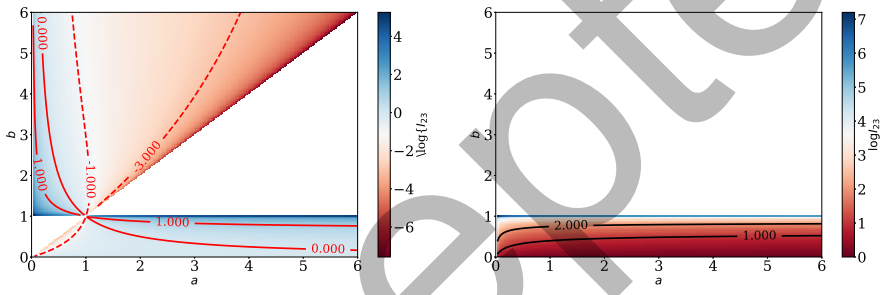

Figure 10: Logarithm of I_{23} for different a and b using the solution of sign "+" (left) and "−" (right).

The interest of these equations yields in the fact that they can be used to calculate the inertial properties of the asteroids —I_{13} and I_{23}— from the characteristics of the rotation speeds that are easily measured: the ratio between ellipse axes and the frequency of the complex velocity W_{12}.

6.1. Numerical examples.

In the previous subsection, it has been shown how the inertia ratios of asteroids can be estimated from their un-relaxed angular velocities. In this section, the accuracy that can be obtained with that approach is studied starting from data of real asteroids' inertia and angular velocities.The objective will not be to get information from a specific asteroid, but to verify that most asteroids meet

García-Gutiérrez, A., Cubas, J., Chen, H., & Sanz-Andrés, Á. (2020).
Complex variable methods for linearized Euler rigid body rotation equations.
Acta Astronautica, 170, 454-465.

the requirements for the use of this method.

In order to obtain real data of inertia matrices and angular velocities of asteroids, the asteroid database DAMIT has been used —acronym of Database of Asteroid Models from Inversion Techniques [17]. For each asteroid —they are around 1600— the database gives its shape, represented as polyhedrons with triangular surface facets. From their shape, using the hypothesis of constant density, their inertial parameters can be calculated. Their real inertia matrices will be slightly different, but this simplification serves as an approximation to the set of inertia matrices of all the asteroids. At this point it is worth remembering that the objective is not to model a particular asteroid, but to know how well the theory works for typical values of inertia and angular velocities than can be found in reality.

The spin states of the different asteroids can be obtained using the parameters of the database; from the light-curves, the radial velocity around the rotational axis can be calculated. All asteroids in the database are supposed to be in a relaxed rotation state [17]. The principal axis with the main moment of inertia calculated using the previous method does not exactly coincide with the axis of rotation. However, this is a necessary requirement for the asteroid to remain relaxed. For this reason, it will be assumed that, before the disturbance, the axis of rotation coincides with the main axis of inertia obtained with the geometric method.

From the relaxed state the inertia ratios cannot be obtained. However, there is the possibility that the asteroid is perturbed by certain mechanisms [18, 19, 20] e.g. outgassing, splitting events, collisions, thermal effects [21] even through controlled impacts like the one proposed in the ESA's Don Quijote Mission [22]. In case of the asteroid being monitored at that time, it would be possible to obtain information about its inertia matrix. To model these mechanisms is beyond the scope of this paper, but the information that can be extracted of a generic disturbance in the form of a random angular velocity variation will be analyzed. For that, a Montecarlo test has been performed as follows:

García-Gutiérrez, A., Cubas, J., Chen, H., & Sanz-Andrés, Á. (2020).
Complex variable methods for linearized Euler rigid body rotation equations.
Acta Astronautica, 170, 454-465.

1. First, a parameter ϵ which characterizes the magnitude of the perturbation in angular velocity is defined. This parameter simulates disturbances of different importance. In this section ϵ is not necessarily small.
2. Then, the absolute value $|\Delta\omega|$ of the perturbation is randomly selected from a normal distribution of mean $\epsilon\langle\omega_3\rangle$ and standar desviation $\epsilon\langle\omega_3\rangle/10$, where $\langle\omega_3\rangle$ denotes the mean ω_3 of the asteroid dataset.
3. Finally, the direction of the perturbation in angular velocity is defined by two angles, $0 < \theta < \pi$ and $0 < \xi < 2\pi$. These angles are also randomly selected. The new angular velocities of the asteroids are computed as: $\omega_1 = \delta\omega_1 = |\Delta\omega|\cos(\xi)\sin(\theta)$, $\omega_2 = \delta\omega_2 = |\Delta\omega|\sin(\xi)\sin(\theta)$ and $\omega_3 = \omega_3 + |\Delta\omega|\cos(\theta)$.

After introducing the perturbation in the angular velocity of the asteroid, each asteroid's attitude is propagated for a period of time equivalent to five rotations, $\Delta T = 10\pi/\omega_{30}$. The Euler equations are numerically integrated —using an explicit Dormand & Price of order 8(5,3), similar to that in Section 4, so the angular velocity components —ω_1, ω_2 and ω_3—are available. Using these results as if they were observational data, the inertia ratios can be estimated as follows:

1. The constant k_m are calculated as the period of $\Omega_{12} = \omega_1 + \mathrm{i}\,\omega_2$. There are several techniques that can be used in order to extract the period from the signal [23]. For simplicity, the fast Fourier transform (FFT) has been used, so the frequency is calculated as the frequency at which the signal spectrum maximum is found.
2. The constant k_c can be found as: $k_c = l_s/s_s$, where l_s is the major semi-axis and s_s the minor semi-axis of the ellipse that Ω_{12} traces in the complex plane. A numerical method to adjust the semi-axis can be found in Fitzgibbon [24].

From k_m and k_c, the estimated inertia ratio I_{13e} and I_{23e} can be computed by using Equations (77a) and (77b). The results can be compared against the inertia ratios used for the simulation.

García-Gutiérrez, A., Cubas, J., Chen, H., & Sanz-Andrés, Á. (2020).
Complex variable methods for linearized Euler rigid body rotation equations.
Acta Astronautica, 170, 454-465.

The results obtained for all the database are shown in Figure 11. For small perturbation $\epsilon < 0.1$, the relative error in the inertia ratios is less than 5% for more than 95% of the cases. The greater the disturbance the more the accuracy is reduced. Nevertheless, the ratio I_{23} is still well estimated even when $\epsilon = 1$ for the 95% of the cases. As it can be seen in this figure, the error is related to the perturbation absolute value. This is a consequence of the linearization done in Eq (60), which requires the perturbation to be small.

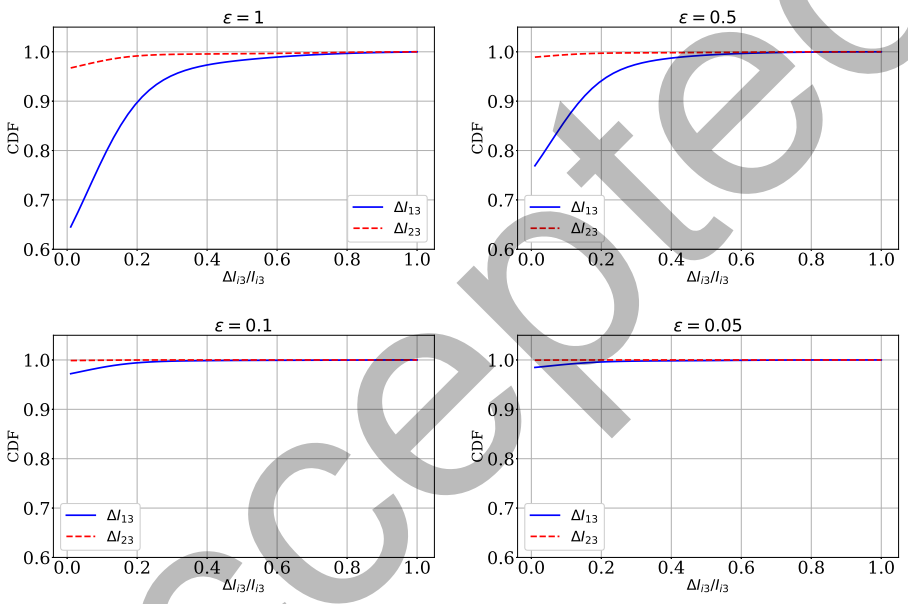

Figure 11: Cummulative distribution function (CDF) of the inertia ratios relative errors $\Delta I_{i3}/I_{i3}$ for different perturbation amplitude, $\epsilon = 1,\ 0.5,\ 0.1$, and 0.05.

In fact, it is not the total magnitude of the disturbance that influences the error, but only the component normal to the axis of rotation, since the perturbation parallel to said axis does not cause any precession or nutation. As shown in Figure 12 —for the case $\epsilon = 0.1$— the joint PDF of the inertia ratio errors depends on the normal velocity perturbations, and reveals a gradual rise in the error as the normal perturbation magnitude increases. In this Figure, each dot represents an asteroid and the PDF isocontour value is 1.0. Technically, this

García-Gutiérrez, A., Cubas, J., Chen, H., & Sanz-Andrés, Á. (2020).
Complex variable methods for linearized Euler rigid body rotation equations.
Acta Astronautica, 170, 454-465.

would indicate that the lower the disturbance the higher the precision that can be obtained with this method. Nevertheless, there is a limit in the resolution of the observation instruments, and this limit would determine the optimal perturbation to minimize the error.

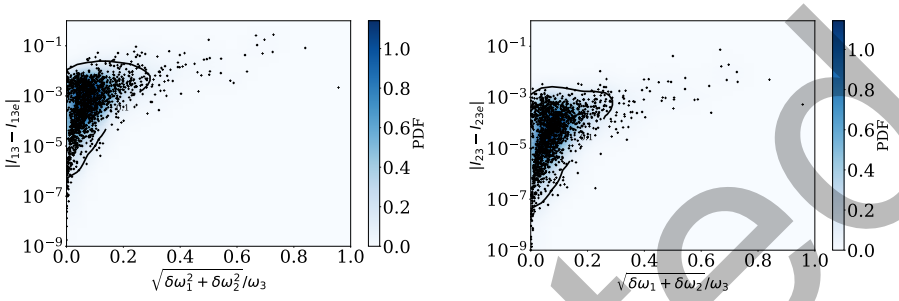

Figure 12: Joint PDF of the inertia error estimation and the simulated normal velocity perturbation. Left image: Absolute error in I_{13}. Right image: Absolute error in I_{23}.

Although the magnitude of the disturbance is clearly the predominant factor in the magnitude of the inertia estimation error, there is still a certain dispersion in the results. This dispersion could be due to other factors such as the shape and inertial matrices of the asteroids. To verify this hypothesis, the correlation between the errors and the moments of inertia of the asteroids has been analyzed.

The inertia ratios of each asteroid in the database is shown in Figure 13 (up) as a point cloud. As can be seen, most asteroids have an ellipsoidal matrix of inertia (I_{13} close to 0.5, I_{23} close to 0.9), with great variety of shapes but few borderline cases. In the same figure (bottom), the 300 asteroids with the largest error estimation are plotted as red squares. Correlations between inertia ratios and errors can be appreciated. In the case of I_{13} estimation error, it is smaller when I_{13} and I_{23} are comparable. And in the case of I_{23} estimation error, it is smaller when I_{13} is close to 0.5. An explanation for these correlations has not been determined yet, but these conclusions can help determine which asteroids are more conducive to applying the proposed method. To highlight these correlations, the Figure 14 has been prepared. In this figure, it can be appreciated that the error in I_{13} grows with the difference $I_{23} - I_{13}$ and, on the

García-Gutiérrez, A., Cubas, J., Chen, H., & Sanz-Andrés, Á. (2020).
Complex variable methods for linearized Euler rigid body rotation equations.
Acta Astronautica, 170, 454-465.

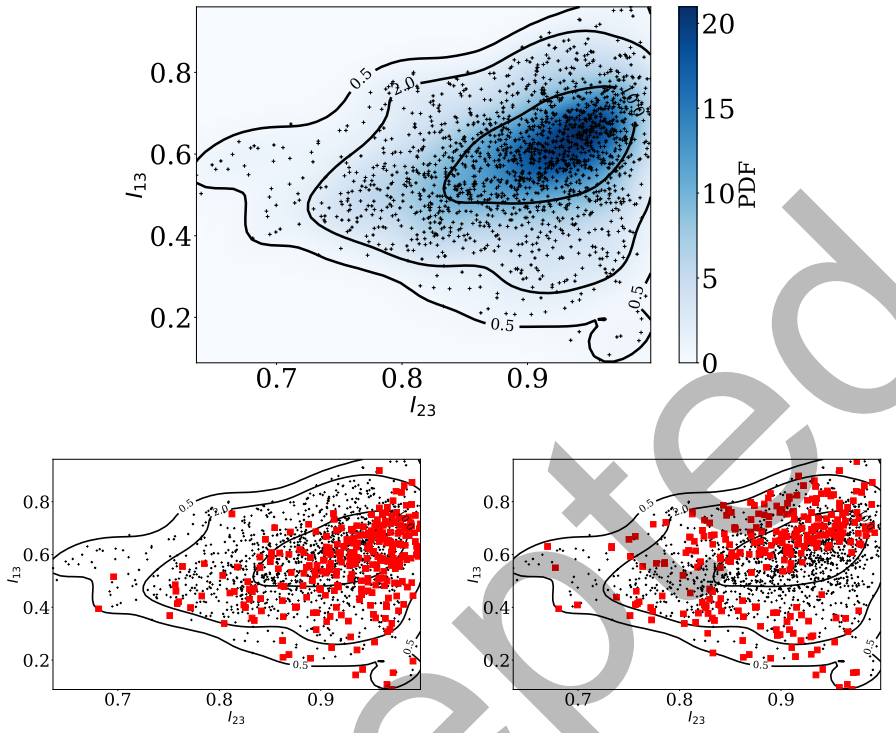

Figure 13: Joint PDF of I_{13} and I_{23}. Isocontour values: 0.5, 2 and 10. Bottom left: 300 asteroids (red squares) with largest error in its I_{13} estimation. Bottom right: 300 asteroids with larger error in its I_{23} estimation.

other hand, the error in I_{23} grows when $|I_{13} - 0.5|$ increases.

7. Conclusions

With the advent of improved computational resources, the use of numerical methods has been growing as a powerful tool used to determine the evolution of complex systems. However, analytic methods still have some useful applications.

In the present study, analytic solutions have been derived for different cases of rigid body rotations that can be typically found in aerospace engineering. In spite of their relevance, a systematic approach to the different problems was not available in the literature. A common methodology is developed for all these

García-Gutiérrez, A., Cubas, J., Chen, H., & Sanz-Andrés, Á. (2020).
Complex variable methods for linearized Euler rigid body rotation equations.
Acta Astronautica, 170, 454-465.

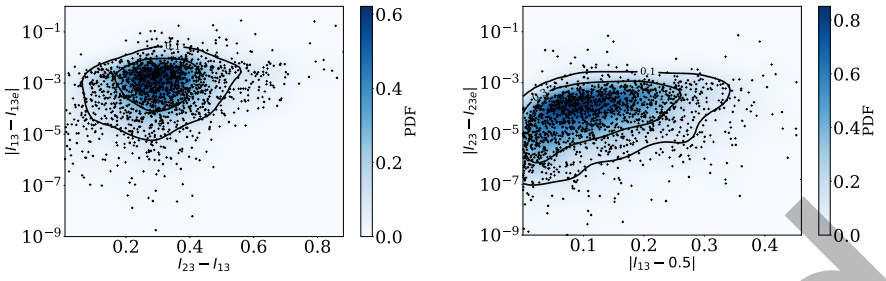

Figure 14: Left image: Joint PDF of the absolute error in I_{13} and the value of $I_{23} - I_{13}$. Right image: Joint PDF of the absolute error in I_{23} and $|0.5 - I_{13}|$. Isocontour values: 0.1 and 0.3.

cases, based on complex variable. The methodology has shown a useful set of characteristics that let us simplify the analytical treatment of the several problems described. Applications of this analytical methodology may include thrust misalignment, sun-tracking attitude motion, response to random/harmonic inputs, stability analysis, etc. This work organize, complements, and extends the contributions of different authors in the literature.

As a particular application, the asteroid attitude has been studied. Due to their low-amplitude rotations, a linearization of the equations can be done not only for the cylindrical inertial tensor but also for the non cylindrical one. In the latter case, new expressions are shown that relate the motion parameters to the inertial ratios of the asteroids and vice versa. That is of particular interest because it opens the possibility of estimating the inertial ratios of the asteroids using only information relative to their motion.

In order to check the utility of the previous linearization, a Montecarlo experiment has been done using the asteroid database DAMIT. In this experiment, the relaxed state of real asteroids is randomly perturbed so the inertial ratios can be calculated using the temporal evolution of the asteroid angular velocities. For perturbations of magnitude $0.1\langle\omega_3\rangle$ —being $\langle\omega_3\rangle$ the mean angular velocity of all the database's comets— the inertia ratios are estimated with a relative error of less than 5% for almost all the asteroids. That error depends on

García-Gutiérrez, A., Cubas, J., Chen, H., & Sanz-Andrés, Á. (2020).
Complex variable methods for linearized Euler rigid body rotation equations.
Acta Astronautica, 170, 454-465.

the magnitude of the perturbation and the asteroid´s inertia matrix although further research should be undertaken to explore and explain the influence of the last one.

Declaration of Competing Interest

The authors declare that there is no conflict of interests regarding the publication of this article.

References

[1] Vladimir S. Aslanov and Vadim V. Yudintsev. Dynamics, analytical solutions and choice of parameters for towed space debris with flexible appendages. *Advances in Space Research*, 55(2):660 – 667, 2015.

[2] Mohammad A. Ayoubi and James M. Longuski. Analytical Solutions for Translational Motion of Spinning-Up Rigid Bodies Subject to Constant Body-Fixed Forces and Moments. *Journal of Applied Mechanics*, 75(1), 01 2008. 011004.

[3] William Tyrrell Thomson. *Introduction to space dynamics*. Courier Corporation, 2012.

[4] Sergey V. Ershkov and Dmytro Leshchenko. On the dynamics of non-rigid asteroid rotation. *Acta Astronautica*, 161:40 – 43, 2019.

[5] David Parry Rubincam. Radiative spin-up and spin-down of small asteroids. *Icarus*, 148(1):2 – 11, 2000.

[6] P. Tsiotras and J. M. Longuski. A complex analytic solution for the attitude motion of a near-symmetric rigid body under body-fixed torques. *Celestial Mechanics and Dynamical Astronomy*, 51(3):281–301, 1991. ID: Tsiotras1991.

[7] P. Tsiotras and J. M. Longuski. Analytic Solution of Euler's Equations of Motion for an Asymmetric Rigid Body. *Journal of Applied Mechanics*, 63(1):149–155, 03 1996.

[8] A. Beck and J. Longuski. *Analytic solution for the velocity of a rigid body during spinning-up maneuvers*. Astrodynamics Conference. American Institute of Aeronautics and Astronautics, 08/01; 2017/04 1994. 01; M1: 0; doi:10.2514/6.1994-3713.

[9] Shota Kikuchi, Kathleen C. Howell, Yuichi Tsuda, and Jun'ichiro Kawaguchi. Orbit-attitude coupled motion around small bodies: Sun-synchronous orbits with sun-tracking attitude motion. *Acta Astronautica*, 140:34 – 48, 2017.

[10] James M. Longuski, R. A. Gick, Mohammad A. Ayoubi, and Laura A. Randall. Analytical solutions for thrusting, spinning spacecraft subject to constant forces. *Journal of Guidance, Control, and Dynamics*, 28(6):1301–1308, 11/01; 2017/05 2005. doi: 10.2514/1.12272; 09.

[11] J. M. Longuski and P. Tsiotras. Analytical solutions for a spinning rigid body subject to time-varying body-fixed torques, part i: Constant axial torque. *Journal of Applied Mechanics*, 60(4):970–975, 12/01 1993. 10.1115/1.2901010.

[12] Mohammad A. Ayoubi, Kaela M. Martin, and James M. Longuski. Analytical solution for spinning thrusting spacecraft with transverse ramp-up torques. *Journal of Guidance, Control, and Dynamics*, 37(4):1272–1282, 2014.

[13] P. Tsiotras and J. M. Longuski. Analytic solutions for a spinning rigid body subject to time-varying body-fixed torques, part ii: Time-varying axial torque. *Journal of Applied Mechanics*, 60(4):976–981, 12/01 1993. 10.1115/1.2901011.

García-Gutiérrez, A., Cubas, J., Chen, H., & Sanz-Andrés, Á. (2020).
Complex variable methods for linearized Euler rigid body rotation equations.
Acta Astronautica, 170, 454-465.

[14] Mohammad A. Ayoubi and James M. Longuski. Asymptotic theory for thrusting, spinning-up spacecraft maneuvers. *Acta Astronautica*, 64(7):810 – 831, 2009.

[15] Julien Frouard and Michael Efroimsky. Precession relaxation of viscoelastic oblate rotators. *Monthly Notices of the Royal Astronomical Society*, 473(1):728–746, Sep 2017.

[16] Sergey V. Ershkov and Roman V. Shamin. The dynamics of asteroid rotation, governed by yorp effect: The kinematic ansatz. *Acta Astronautica*, 149:47 – 54, 2018.

[17] J. Durech, V. Sidorin, and M. Kaasalainen. DAMIT: a database of asteroid models. *Astronomy and Astrophysics*, 513:A46, April 2010.

[18] Nalin H Samarasinha, Béatrice EA Mueller, Michael JS Belton, and Laurent Jorda. Rotation of cometary nuclei. *Comets II*, pages 281–299, 2004.

[19] Roman R. Rafikov. Spin evolution and cometary interpretation of the interstellar minor object 1i/2017 'oumuamua. *The Astrophysical Journal*, 867(1):L17, Oct 2018.

[20] Roman R. Rafikov. Non-gravitational forces and spin evolution of comets, 2018.

[21] David Vokrouhlickỳ, David Nesvornỳ, and William F Bottke. The vector alignments of asteroid spins by thermal torques. *Nature*, 425(6954):147, 2003.

[22] Andrés Gálvez and Ian Carnelli. ESA's Don Quijote Mission: an opportunity for the investigation of an artificial impact crater on an asteroid. In *25th International Symposium on Space Technology and Science*, 2006.

[23] B. G. Quinn and E. J. Hannan. *The Estimation and Tracking of Frequency*. Cambridge Series in Statistical and Probabilistic Mathematics. Cambridge University Press, 1 edition, 2001.

García-Gutiérrez, A., Cubas, J., Chen, H., & Sanz-Andrés, Á. (2020).
Complex variable methods for linearized Euler rigid body rotation equations.
Acta Astronautica, 170, 454-465.

[24] A. W. Fitzgibbon, M. Pilu, and R. B. Fisher. Direct least squares fitting of ellipses. In *Proceedings of 13th International Conference on Pattern Recognition*, volume 1, pages 253–257 vol.1, Aug 1996.